ChemPubSoc Europe

DOI: 10.1002/slct.201903396

Chemistry SELECT Full Papers

Materials Science inc. Nanomaterials & Polymers

Gold Nanoparticles Stabilized by Sulfonated-Imidazolium Salts as Promising Catalyst in Water

Gustavo A. Monti,[a] N. Mariano Correa,[a] R. Darío Falcone,[a] Gustavo F. Silbestri,*[b] and Fernando Moyano*[a]

We present the total characterization (by FT-IR and NMR spectroscopies) of gold nanoparticles (Au-NPs) stabilized by different sulfonated-imidazolium salts. Also, thermogravimetric analysis (TGA) was used in order to evaluate the degree of the Au-NPs coverage. Our results show how the orientation of the sulfonated-imidazolium salts and, the interaction of the hydrocarbon chain with the Au-NP surface are responsible for the strength of the ligand-Au-NP interaction. The developed procedure is easy, fast and reproducible to carry out different catalytic organic reactions in water. Our preliminary studies indicate that Au-NPs synthesized are active and recyclable catalysts for the reduction of aromatic nitro compounds at room temperature in water.

Introduction

Currently, the interest in imidazole derivatives is based on the generation of carbenes, motivated by the isolation, in 1995, of the first stable compound.[1] Their chemical and physical properties can be adjusted to a wide range of applications varying the cations and anions. Generally, the anion has a greater influence on the property of the imidazolium salt.[2] In this sense a new type of salts, such as zwitterions composed of covalently bonded cations and anions, has been developed.[3] It should be mentioned that Dupont *et al.* have suggested that the intrinsic charge, combined with the steric volume of the imidazolium salts, which can be described as supramolecular polymers with weak interactions, can create an electrostatic and steric colloidal stabilization with transition metal nanoparticles (M-NPs).[4]

The discovery that imidazolium salts can act as new media for the preparation and stabilization of M-NPs is quite casual. It began with the isolation of NPs during catalytic hydrogenation and C–C coupling reactions using organometallic compounds or metal salts in ionic liquids (ILs). For example, Deshmukh *et al.* have performance reactions using palladium catalysts [Pd $(AcO)_2$ and $PdCl_2$] in 1,3-dibutylimidazolium bromide under ultrasonic irradiation conditions, observing the formation of Pd-NPs of 20 nm composed of nanoclusters of 1 nm, formed by the reduction of Pd^{+2}.[5] Hamill *et al.* detected the formation of Pd clusters of 0.8-1.6 nm during the Heck reaction using several ILs.[6] Among the first publications in this field, Dupont synthesized uniform size Ir-NPs and used them as catalysts for olefins hydrogenation.[4] This pioneering work stimulated many subsequent studies, leading to the synthesis of Ir-,[7] Pt-,[8] Ru-,[9] Pd-,[10] Ni-,[11] Cu-,[12] and Ag-NPs[13] by reducing the corresponding metal salts or by means of the decomposition of organometallic compounds in different ILs.[14]

It is noteworthy that this type of compounds -imidazolium salts- act as stabilizing agents in the synthesis of M-NPs without the presence of a traditional stabilizing agent. One way of stabilizing NPs is usually achieved with the use of ligands, which fulfill a triple function: to avoid agglomeration between the particles, to decrease the surface energy and to act as a physical barrier to reduce the diffusion of species to the particle surface. There are at least two types of well-differentiated interactions between ligands-NPs; On one side, there are ligands that interact covalently with the surface of the NP[15] : this allows to control the stability of the dispersions of the steric properties of the stabilizer while imparting their characteristics and properties to the modified NPs. On the other side, there are those ligands that have charge, which stabilize the NPs by means of the Coulomb repulsion between the diffuse layers of the NP and the stabilizer.[16]

In recent years, Au-NPs have acquired an important role in the field of nanomaterials.[17] It is very interesting to study these NPs since some of them are compatible with biomolecules, which are useful for applying them in the field of biomedicine,[18] including sensors,[19] images for therapies against cancer,[20] etc. On the other hand, the number of reports on the use of Au-NPs, as catalysts of different organic reactions, has grown considerably.[21] Specially in oxidation,[22] hydrogenation,[23] and cross-coupling reactions.[24]

As has been summarized, there is clear evidence that demonstrates the potential of imidazole derivatives for being prepared and stabilized M-NPs in aqueous media. In this sense and continuing with our investigations in this topic,[25] now we

[a] *G. A. Monti, Prof. N. M. Correa, Dr. R. D. Falcone, Dr. F. Moyano*
Instituto para el desarrollo agroindustrial y de la salud, IDAS, (CONICET – UNRC.) Departamento de Química. Universidad Nacional de Río Cuarto. Agencia Postal # 3. C.P. X5804BYA Río Cuarto, Argentina
E-mail: fmoyano@exa.unrc.edu.ar

[b] *Dr. G. F. Silbestri*
Instituto de Química del Sur (INQUISUR), Departamento de Química, Universidad Nacional del Sur (UNS)-CONICET, Av. Alem 1253, B8000CPB Bahía Blanca, ArgentinaSupporting information for this article is available on the WWW underhttps://doi.org/10.1002/slct.201903396
E-mail: gsilbestri@uns.edu.ar

extend the physical-chemical study of the role that a series of sulfonated-imidazolium salts **Lx** [1,3-bis(2,6-diisopropyl-4-sodiumsulfonatophenyl)imidazolium (**L1**), 1-mesityl-3-(3-sulfonatopropyl)imidazolium (**L2**) and 1-(3-sulfonatopropyl)imidazolium (**L3**), Scheme 1] fulfill in the stabilization of Au-NPs. A brief description of the synthesis of sulfonated-imidazolium salts is shown in the Supporting Information.

Recently,[25] Au-NPs stabilized with the imidazolium salts (Au-NPs:**Lx**, see Supporting Information) by different techniques such as UV-Vis spectroscopy, transmission electron microscopy (TEM), dynamic light scattering (DLS) and, Zeta potential were partially characterized. These NPs were stabilized by electrostatic interaction between the imidazolium salts and the surface of NP. All NPs have negative values of zeta potential and this is due to the sulfonated group of the different salts. The size found of different the Au-NP stabilized in water by TEM was 9 nm for **L1**, 15 nm for **L2** and 13 nm for **L3**. These values were consistent with determinate by DLS. However, how is the strength of the ligand-NPs interaction, what is the orientation of the sulfonated imidazolium salts over the particle and, which is the cover grade, are questions that we will answer in this work since these are crucial issues in order to use Au-NPs in different chemistry fields. In this sense, aromatic nitro compounds are part of the chemical formulation of different pesticides.[26] These constitute a risk to health if they are found in water sources since they are capable of causing diseases such as cyanosis and anemia.[27] In contrast, aminobenzenes are less toxic, but not harmless, because some can be metabolized and excreted in urine.[27]

Results and discussion

In order to evaluate the strength of the ligand-NPs interaction, the orientation of the sulfonated imidazolium salts over the particle and the cover grade, we have used FT-IR spectroscopy, ^{1}H NMR, and TGA techniques. Moreover, synthesized Au-NPs were used to demonstrate the catalytic power for the reduction of aromatic nitro compounds in water.

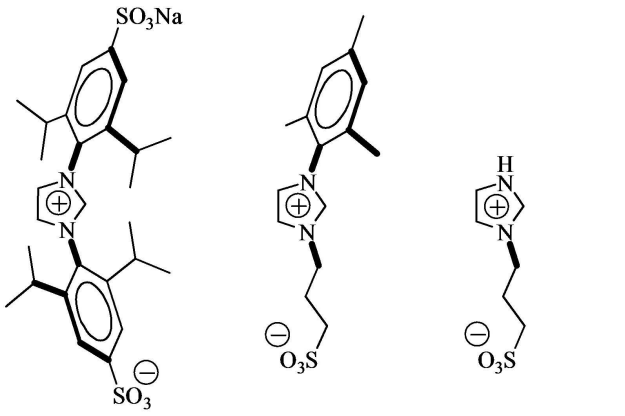

L1 573.72 g/mol **L2** 311.42 g/mol **L3** 193.24 g/mol

Scheme 1. Chemical structure of Sulfonated-imidazolium salts (**Lx**) and their corresponding Molecular weight.

FT-IR spectroscopy

Imidazolium group

For the ILs composed of 1-alkyl-3-methyl imidazolium, the infrared bands found between 3200 and 3100 cm^{-1} are assigned to the aromatic C–H stretching modes of C^2-H and C^{4,5}-H on the imidazolium cation.[28,29] The band at lower frequency is assigned to the C^2-H stretching modes because the group has a larger positive charge density than the C^{4,5}-H groups, which leads to smaller force constants.[30]

The bands of the most relevant stretching modes for sulfonated-imidazolium salts were identified by FT-IR (see Figure S1 and Table S1 in the Supporting Information). However, in order to simplify the analysis we decide to center our investigations in a few distinguish bands, such as the aromatic C^2-H of the imidazolium cation and the corresponding to the sulfonate anion. Please refer to Table S1 to see the atoms labels.

Figure 1A shows the FT-IR spectra corresponding to the aromatic C^2-H stretching mode of the pure salt **L1** (ν_{max} = 3075 cm^{-1}, black line) and **L1** in the presence of Au-NPs (ν_{max} = 3033 cm^{-1}, red line). As can be seen, there is a change in both: the position and the shape of the bands. Profiles similar was found by Holze *et.al.*[31] by using near-infrared surface-enhanced Raman Scaterring (NIR-SERS) for imidazole on gold, specifically on the surface of an Au electrode. Particularly, ours result shows that there is a noticeable-broadening of the bands when the salt is stabilizing the NP. On the other hand, the bands appear at lower frequencies, and this shift is caused by interactions that modify the charge density of the imidazole ring due to i) the interaction with the gold surface and/or ii) the proximity of a sulfonate group of another molecule and/or iii) the interaction with the π electrons.

However, as can be seen in Figures 1B and C, the interaction between the imidazolium salts, **L2** (ν_{max} = 3106 cm^{-1}) and **L3** (ν_{max} = 3116 cm^{-1}), and the NP surface is different (ν_{max} = 3132 cm^{-1} and 3144 cm^{-1}, respectively). In both salts, the interaction with the NP causes an increase in the positive charge density of the imidazole ring that makes the C^2-H bond become stronger, and consequently appears at higher frequencies than pure salt.

Sulfonate group

The SO_3^- stretching vibrations were investigated earlier by infrared spectroscopy[32,33] and the SO_3 asymmetric stretching mode was observed at 1320–1200 cm^{-1}. This SO_3 stretching region provides important information about the strength of cation-anion interactions. With regard to the stretching modes of the sulfonate group, Li *et al.*[34] have described that when the sulfonate group interacts with a cation, the symmetry corresponding to that stretch decreases which causes the band to split.[35] On the other hand, the magnitude in the separation of the band indicates the strength in the electrostatic interaction between the sulfonate group and the cation.[36]

Figure 2 shows the FT-IR spectra of **L3** and the Au-NPs:**L3** in the spectral region between 1270–1120 cm^{-1} and 1070–

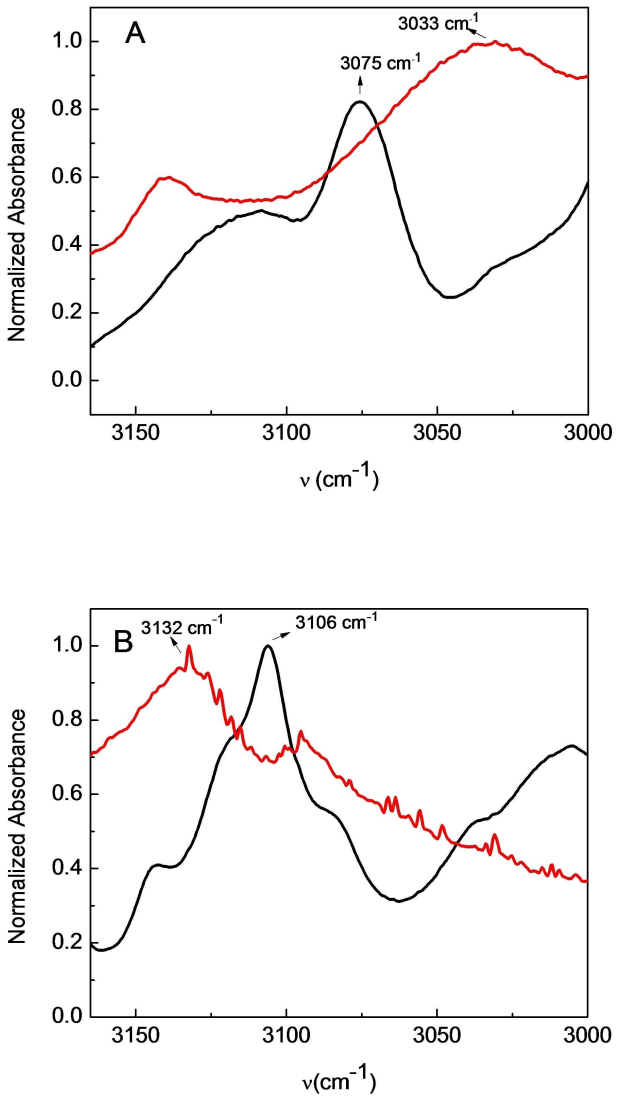

Figure 1. FT-IR spectra corresponding to the aromatic C^2-H stretching region of the imidazolium ring in the pure salts **Lx** (black line) and Au-NPs:**Lx** (red line). (A) **L1**, (B) **L2** and, (C) **L3**.

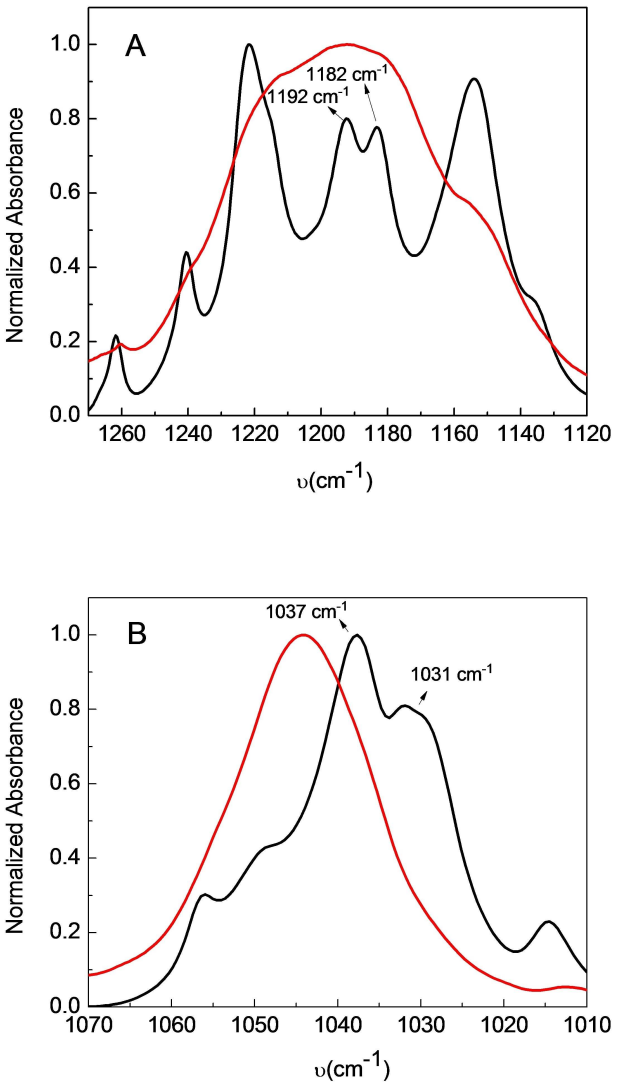

Figure 2. FT-IR spectra of stretching of sulfonate group of **L3** (black line) and Au-NPs:**L3** (red line). (A) Asymmetric, (B) Symmetric.

1010 cm^{-1} for the asymmetric (A) and symmetrical (B) stretching S=O bond of the sulfonate group, respectively. As can be seen in Figure 2A, the absorption band corresponding to **L3** (black line) splits in two sharp peaks centered at 1192 and 1182 cm^{-1}, respectively. This splitting was attributed to the change in the molecular symmetry of the vibration of the sulfonate group due to the electrostatic interaction that exists between the sulfonate anion and the imidazolium cation of the zwitterionic compound.[36–38] However, the same absorption band corresponding to Au-NPs:**L3** (red line) became a broad-band centered around 1200 cm^{-1}. This drastic change in the shape of the band could be due to the fact that the ligand interacts through the imidazolium cation with the surface of the Au-NPs, invoked before.

On the other hand, the band corresponding to the symmetric vibration mode of sulfonate group in **L3** (Figure 2B, black line) splits into a sharp peak at 1037 cm^{-1} and a "shoulder" at 1031 cm^{-1}, which shows, again, that the sulfonate

group also interacts electrostatically with the imidazolium cation. Similar to the asymmetric vibration, when **L3** acts as a ligand for the NP, an enveloping band with a maximum of 1045 cm^{-1} is observed. Similar conclusions can be invoked from the asymmetric and symmetric stretching modes of the sulfonate group, of **L1**, **L2**, Au-NPs:**L1**, Au-NPs:**L2**, using FT-IR technique (see Figure S2, Supporting Information).

^{1}H NMR spectroscopy

One of the questions that we have not been able to answer so far is to determine the spatial arrangement of the imidazolium salts in the interaction of NP (Au-NP: **Lx**). To solve this question, ^{1}H NMR experiments were performed. All ^{1}H NMR spectra for **Lx** and Au-NP: **Lx** are shown in Figure S3 (Supporting Information) and the chemical shifts are summarized in Table 1.

In the ^{1}H NMR spectrum of the imidazolium salt **L1** (Figure S3a), the H signals of the imidazolium ring appear at 9.58, 7.96 and 7.95 ppm, while the position of these signals in the Au-NP: **L1** is quite small and, probably, not very significant (9.63, 8.01 and 8.00 ppm, respectively). In addition, the position of the H of the isopropyl and phenyl groups changes towards δ higher for the Au-NP: **L1** (1.21 and 1.12 ppm) with respect to **L1** (1.14 and 1.05 ppm). These displacements are consequence of the change in the electronic environment that seems to affect the salt when interacts with the NP surface. Apparently, the isopropyl groups would act as a steric barrier preventing that the imidazolium cation to approach the surface of gold. Consequently, the imidazolium cation has a lower positive charge density with respect to pure **L1**, due to its greater availability of π electrons in the ring.[39,40] The NMR behavior observed in this case is consistent with the study of noble metal nanoparticle growth, surface chemistry, and physical properties observed by Shi *et al.*[41] and, Millstone *et al.*[42]

As shown in Table 1, for **L3** and Au-NP: **L3** the scenario is completely different. The metal-ligand interaction produces an increase in the positive charge density of the imidazole cation due to the repulsion that exists between the gold surface and the imidazole ring. This shielding causes the signal of the H of the rings to appear at lower δ (8.67, 7.47 and 7.39 ppm for **L3** and 8.27, 7.32 and 7.21 ppm for Au-NPs: **L3**, respectively). The same effect is observed for H of the aliphatic chain (See Table 1). These results are in agreement with that found by FT-IR spectroscopy. The C^2-H stretch of the Au-NPs: **L3** appears at higher frequencies than the stretch of pure **L3** (Figure 1C), indicating an imidazolium cation with a higher positive charge density.

Now, we focus our attention on the H of the aliphatic chains for **L2**, **L3**, and their respective Au-NPs:**Lx**. While there are no appreciable changes for **L2** and its respective Au-NPs:**L2**, it is notorious the displacement to high fields of the aliphatic H signals of **L3** (4.35, 2.84 and 2.25 ppm) when stabilizing the Au-NPs (4.24, 2.78 and 2.19 ppm) indicating a greater approach of the alkyl chain to the metal surface.

These results show that the strength of the interaction between the ligand surface and gold NP depends on the chemical structure of the stabilizer. Probably, the steric hindrance of the imidazolium salts (**L1** > **L2** > **L3**) is the determining factor.

Table 1. ^{1}H NMR Chemical shifts of imidazolium salts and stabilized Au-NPs (Au-NPs:**Lx**) in D_2O.

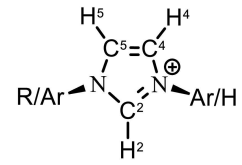

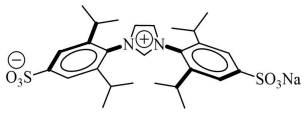

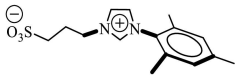

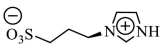

	L1	Au-NPs(L1)	L2	Au-NPs(L2)	L3	Au-NPs(L3)
NC^2*H*^{2}N	9.58	9.63	8.97	8.91	8.67	8.27
Ar,Imz C^4*H*^{4}	7.96	8.01	7.75	7.73	7.47	7.32
Ar,Imz C^5*H*^{5}	7.95	8.00	7.51	7.48	7.39	7.21
Ar	7.71	7.76	7.07	7.06	–	–
NC*H*$_2$	–	–	4.30	4.41	4.35	4.24
SC*H*$_2$	–	–	2.85	2.87	2.84	2.78
CH$_2$*CH*$_2$CH$_2$	–	–	2.38	2.33	2.25	2.19
p-*Me*Ar	–	–	2.25	2.25	–	–
o-*Me*Ar	–	–	1.96	1.94	–	–
***CH*Me$_2$**	2.36	2.42	–	–	–	–
CH*Me*$_2$	1.14	1.21	–	–	–	–
CH*Me*$_2$	1.05	1.12	–	–	–	–
NH	–	–	–	-	n.o.	n.o.

n.o.: not observed.

TGA technique

Figure 3 shows profiles of the TGA measurements for the different Au-NPs:**Lx**. It is necessary to remark that the organic matter percentage determination by TGA technique correspond to **Lx**. Note, that the profile of Au-NPs:**L1** is different from Au-NPs:**L2** and, Au-NPs:**L3** and, this could be possibly due to the fact that the salt decomposes before it melts.

In the Figure 3, it is observed that there are stages corresponding to a water loss (50 °C-150 °C) due to the desorption of the water molecules on the surface of the NPs. Also, the degree of coverage on Au-NP surfaces with the different **Lx** can be appreciated. That is, we have observed the total weights of the imidazolium salt fraction in the Au-NP are different. The results found are 59%, 67% and 48% to Au-NPs: **L1**, Au-NPs:**L2** and, Au-NPs:**L3**, respectively.

Then, it is possible to perform a study and obtain the average number of the salt present on the NP core in each Au-NPs as it was explained in the experimental section.[43,44] In Table 2, we have provided the values of $N°_{Au}$, the weight of the Au-NPs, the weight of the imidazolium salt fraction, and the average number of salt around Au-NPs, determined as described in the Experimental section. It is interesting to make an analysis of the value obtained when the NPs are comparable in size that is **L2** and **L3**.

Table 2 shows that the N° of **Lx** per Au-NPs obtained by **L3** is smaller compared to **L2**. This can be explained because a different spatial arrangement in comparison with **L2** causes that approximately 33852 molecules cover the Au-NPs. This asseveration comes from the ^{1}H NMR data where it was detected interaction between the aliphatic chains of **L3** with the NPs surface. This makes that the orientation of **L3** on the Au-NPs surface is different compared with **L1** and **L2** (Scheme 2). In **L3**, the protons of the imidazole ring (2, 4 and 5) are the ones that experiment stronger interaction with the NPs (major changes in the signal) in comparison with the other ligands. Therefore, this salt approaches the NPs through the imidazole ring. In addition, the protons signals of the alkyl chain are modified indicating that the side chain folds over the NPs.

On the other hand, the same protons signals (2, 4 and 5) in **L1** and **L2** do not seems to be modified. In the case of **L1** the isopropyl groups exert a steric barrier (the signals corresponding to that group are modified) and, in the case of the **L2**, the proton signals of the side chain are not so influenced by the metal indicating that the distance to the NPs is far. Finally, although, **L2** behaves similarly to **L3** in FT-IR spectra (C2-H stretching mode shift to higher frequencies in the Au-NPs in respect to the free imidazolium salts) and by ^{1}H NMR, the imidazolium ring (2, 4 and 5) shift to high field in both cases. It important to note that, in **L2** the changes in the imidazolic protons are minor indicating that the ring does not interact directly with the NPs as **L3** does. We consider that mesityl group (2,4,6-trimethylphenyl) is located in such a way that the alkyl chain is detached from the metal surface, however, there are no appreciable changes in the chemical shifts of these signals. In addition, a complete theoretical analysis of the spatial arrangement of salts around the nanoparticle is currently ongoing and will be published in due course.

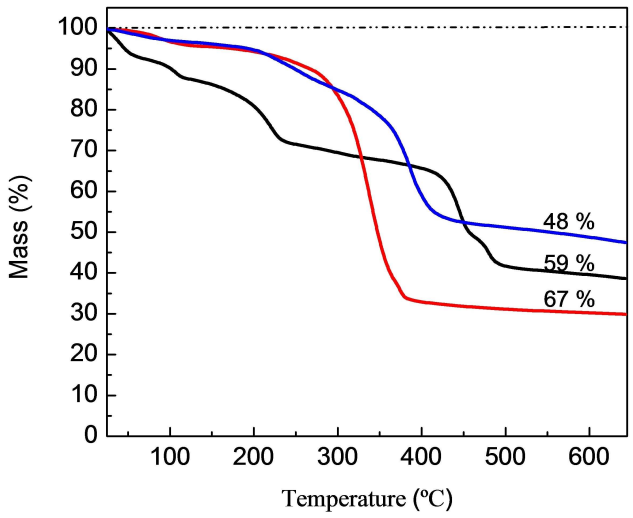

Figure 3. TGA of Au-NPs stabilizer with different **Lx**. Au-NPs:**L1** (black line), Au-NPs:**L2** (red line) and Au-NPs:**L3** (blue line), respectively.

Table 2. Calculated Au-NPs parameters stabilizer by different Imidazolium salt.

	Au-NPs: L1	Au-NPs: L2	Au-NPs: L3
Diameters (nm)	9	15	13
$N°_{Au}$	22520	104253	67870
Weight of Au-NPs core*	$4.44x10^6$	$2.05x10^7$	$1.34x10^7$
Organic fraction (%)	59	67	48
Weight of organic fraction*	$6.39x10^6$	$4.16x10^7$	$1.24x10^7$
Average number of **Lx** per Au-NPs	11138	133582	64169
Number of **Lx** per nm^2	44	189	121

*Atomic and molecular weights are given in Dalton.

Reduction of aromatic nitro compounds in water.

Finally, as an interesting example of future applications of the Au-NPs:**Lx**, preliminary and exciting results about the catalytic effect that the NPs have for the reduction of 1,4-dinitrobenzene at room temperature in water have been obtained. Figure 4

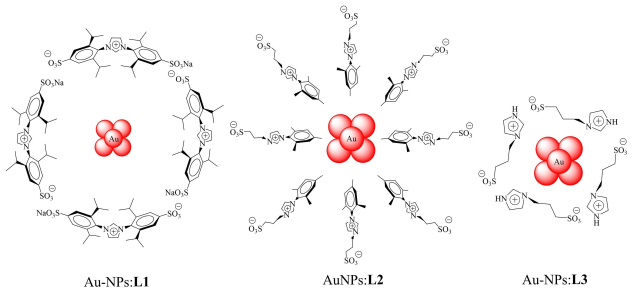

Scheme 2. Hypothetic spatial arrangement of the different imidazolium salts around the Au-NPs.

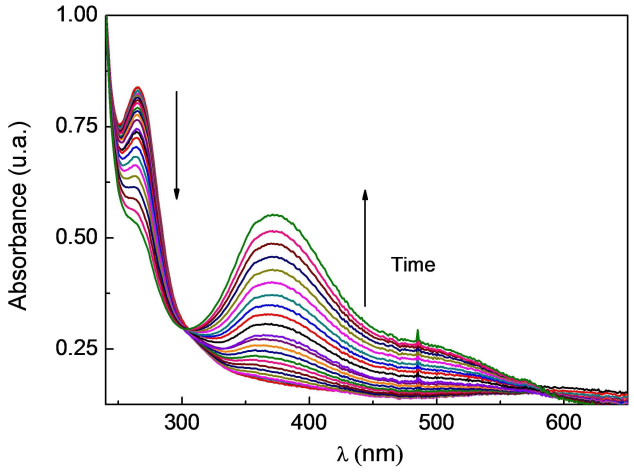

Figure 4. Absorption spectra at different times of the reaction between 1,4-dinitrobenzene and hydrazine in water catalyzed by Au-NPs:**L1**. [1,4-dinitrobenzene] = $5x10^{-5}$M, [hydrazine] = 0.1 M and [Au-NPs] = $1x10^{-8}$ M. Time: 0 s (black line) until 1756 s (green line).

shows typical absorption spectra of the reduction of 1,4-dinitrobenzene to 4-nitroaniline using Au-NPs:**L1** as catalyst (Scheme 3) at different reaction time.

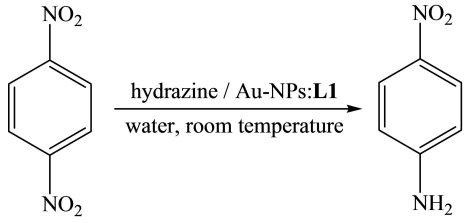

Scheme 3. Reduction of 1,4-dinitrobenzene using Au-NPs:**L1** as catalyst.

The absorption spectra of the reaction show a clear isosbestic point (λ = 303 nm), evidencing the lack of intermediates and/or product decomposition. There is an increase in the absorbance values at different reaction times at λ = 373 nm which correspond to the formation of the product 4-nitroaniline.

All Au-NPs:**Lx** were active after 30 min at room temperature with an Au loading of $1x10^{-8}$ M. Recovery experiments showed high levels of recyclability (4 cycles). It is important to mention the absence of colloidal Au particles in aqueous solutions at the end of the catalyzed reactions that suggest that the NPs are stable under the reaction conditions used.

Conclusions

Here we describe a detailed physicochemical characterization of Au-NPs synthesized in water, using different sulfonated imidazolium salts as stabilizers. The Au-NPs were characterized -with an excellent agreement between the different techniques- by FT-IR and ^{1}H NMR spectroscopies. In addition, TGA was used to determine the degree of coverage of the Au-NPs by the ligands.

Our results reveal that Au-NPs interact electrostatically with imidazolium salts through the imidazolium ring. The orientation of the sulfonate groups and the hydrocarbon chain are responsible for the strength of the ligand-Au-NP interaction and, consequently, the stability of the Au-NP dispersed in water. For the **L1** salt, the interaction with Au-NPs is perturbed by the isopropyl group, which decreases the charge density of imidazolium ring and, consequently, make that the Au-NPs surface to have less coverage. The coverage of the nanoparticles for both salts, **L2** and **L3**, is greater compared to **L1**. For the **L3** salt, a greater proximity of the alkyl chain on the surface of Au-NP was detected, indicating that the orientation and coverage in Au-NPs is different compared to **L2**.

Preliminary studies show that the synthesized Au-NPs:**Lx** are active and recyclable catalysts for the reduction of nitroaromatic compounds in water. Further work is in development in our laboratories focusing on the reactivity of these water-soluble Au-NPs.

Supporting Information Summary.

Supporting information PDF file contains experimental procedures and, Figures and Tables from where the shifts ^{1}H NMR and FT-IR spectroscopies were obtained.

Acknowledgements

Financial support from the Consejo Nacional de Investigaciones Científicas y Técnicas, Universidad Nacional de Río Cuarto, Universidad Nacional del Sur, Agencia Nacional de Promoción Científica y Técnica (PICT-2015-2151 and PICT-2015-0585), and Ministerio de Ciencia y Tecnología, Gobierno de la provincia de Córdoba is gratefully acknowledged. N.M.C., R.D.F., F.M. and, G.F.S. hold a research position at CONICET. G.M. thanks from CONICET for a research doctoral fellowship. Last, but not least, we thank one anonymous reviewer for his/her invaluable and constructive input.

Conflict of Interest

The authors declare no conflict of interest.

Keywords: catalyst · FT-IR · gold nanoparticle · ^{1}H-NMR · sulfonated-imidazolium salts

[1] A. J. Arduengo, J. R. Goerlich, W. J. Marshall, *J. Am. Chem. Soc.* **1995**, *117*, 11027–11028.
[2] I. López-Martin, E. Burello, P. N. Davey, K. R. Seddon, G. Rothenberg, *ChemPhysChem* **2007**, *8*, 690–695.
[3] A. D. Mc Naught, A. Wilkinson, *IUPAC Compend. Chem. Terminol.* **1997**, 1598.
[4] J. Dupont, G. S. Fonseca, A. P. Umpierre, P. F. P. Fichtner, S. R. Teixeira, *J. Am. Chem. Soc.* **2002**, *124*, 4228–4229.
[5] R. R. Deshmukh, R. Rajagopal, K. V. Srinivasan, *Chem. Commun.* **2001**, 1544–1545.

[6] N. A. Hamill, C. Hardacre, S. E. J. McMath, *Green Chem.* **2002**, *4*, 139–142.
[7] G. S. Fonseca, A. P. Umpierre, P. F. P. Fichtner, S. R. Teixeira, J. Dupont, *Chem. Eur. J.* **2003**, *9*, 3263–3269.
[8] C. W. Scheeren, G. Machado, J. Dupont, P. F. P. Fichtner, S. R. Texeira, *Inorg. Chem.* **2003**, *42*, 4738–4742.
[9] S. Miao, Z. Liu, B. Han, J. Huang, Z. Sun, J. Zhang, T. Jiang, *Angew. Chem. Int. Ed.* **2005**, *45*, 266–269.
[10] V. Caló, A. Nacci, A. Monopoli, S. Laera, N. Cioffi, *J. Org. Chem.* **2003**, *68*, 2929–2933.
[11] P. Migowski, G. Machado, S. R. Texeira, M. C. M. Alves, J. Morais, A. Traverse, J. Dupont, *Phys. Chem. Chem. Phys.* **2007**, *9*, 4814–4821.
[12] P. Singh, A. Katyal, R. Kalra, R. Chandra, *Tetrahedron Lett.* **2008**, *49*, 727–730.
[13] K.-S. Kim, D. Demberelnyamba, H. Lee, *Langmuir* **2004**, *20*, 556–560.
[14] J. Dupont, D. De Oliveira Silva, *Nanoparticles Catal.* **2008**, 195–218.
[15] J. M. Asensio, S. Tricard, Y. Coppel, R. Andrés, B. Chaudret, E. de Jesús, *Chem. Eur. J.* **2017**, *23*, 13435–13444.
[16] H. S. Schrekker, M. A. Gelesky, M. P. Stracke, C. M. L. Schrekker, G. Machado, S. R. Teixeira, J. C. Rubim, J. Dupont, *J. Colloid Interface Sci.* **2007**, *316*, 189–195.
[17] S. Alex, A. Tiwari, *J. Nanosci. Nanotechnol.* **2015**, *15*, 1869–1894.
[18] P. K. Jain, K. S. Lee, I. H. El-Sayed, M. A. El-Sayed, *J. Phys. Chem. B* **2006**, *110*, 7238–7248.
[19] K. Saha, S. S. Agasti, C. Kim, X. Li, V. M. Rotello, *Chem. Rev.* **2012**, *112*, 2739–2779.
[20] X. Huang, I. H. El-Sayed, W. Qian, M. A. El-Sayed, *J. Am. Chem. Soc.* **2006**, *128*, 2115–2120.
[21] A. Wittstock, V. Zielasek, J. Biener, C. M. Friend, M. Bäumer, *Science* **2010**, *327*, 319–322.
[22] T. S. G. Dorda, M. Pepper, A. Karlhede, S. A. Kivelson, E. H. Rezayi, A. H. Macdonald, E. Tutuc, S. J. Papadakis, M. Shayegan, *Science* **2006**, 332–335.
[23] M. Turner, V. B. Golovko, O. P. H. Vaughan, P. Abdulkin, A. Berenguer-Murcia, M. S. Tikhov, B. F. G. Johnson, R. M. Lambert, *Nature* **2008**, *454*, 981–983.
[24] P. D. Stevens, J. Fan, H. M. R. Gardimalla, M. Yen, Y. Gao, *Org. Lett.* **2005**, *7*, 2085–2088.
[25] G. A. Monti, G. A. Fernández, N. M. Correa, R. D. Falcone, F. Moyano, G. F. Silbestri, *R. Soc. Open Sci.* **2017**, *4*, 170481–170491.
[26] Y. Keum, Q. X. Li, *Chemosphere* **2004**, *54*, 255–263.
[27] Å. Wennmalm, G. Benthin, A. Edlund, L. Jungersten, N. Kieler-Jensen, S. Lundin, U. N. Westfelt, A. S. Petersson, F. Waagstein, *Circ. Res.* **1993**, *73*, 1121–1127.
[28] J.-C. Lassègues, J. Grondin, D. Cavagnat, P. Johansson, *J. Phys. Chem. A* **2009**, *113*, 6419–6421.
[29] J. Shi, P. Wu, F. Yan, *Langmuir* **2010**, *26*, 11427–11434.
[30] R. M. Silverstein, F. X. Webster, D. J. Kiemle, *Spectrometric Identification of Organic Compounds*, State University of New York College of Environmental Science and Forestry, **2005**, 369.
[31] R. Holze, *Electrochim. Acta* **1993**, *38*, 947–956.
[32] A. Bernson, J. Lindgren, *Polymer (Guildf).* **1994**, *35*, 4842–4847.
[33] J. M. Andanson, F. Jutz, A. Baiker, *J. Supercrit. Fluids* **2010**, *55*, 395–400.
[34] Q. Li, S. Weng, J. Wu, N. Zhou, *J. Phys. Chem. B* **1998**, *102*, 3168–3174.
[35] J. M. Alía, H. G. M. Edwards, *Vib. Spectrosc.* **2000**, *24*, 185–200.
[36] P. D. Moran, G. a Bowmaker, R. P. Cooney, *Langmuir* **1995**, *11*, 738–743.
[37] P. D. Moran, G. A. Bowmaker, R. P. Cooney, J. R. Bartlett, J. L. Woolfrey, *J. Mater. Chem.* **1995**, *5*, 295–302.
[38] C. M. O. Lépori, N. M. Correa, J. J. Silber, F. Vaca Chávez, R. D. Falcone, *Soft Matter* **2019**, *15*, 947–955.
[39] G. A. Fernández, A. B. Chopa, G. F. Silbestri, *Catal. Sci. Technol.* **2016**, *6*, 1921–1929.
[40] G. A. Fernández, V. Dorn, A. B. Chopa, G. F. Silbestri, *J. Organomet. Chem.* **2017**, *852*, 20–26.
[41] B. Zhou, L. Zheng, C. Peng, D. Li, J. Li, S. Wen, M. Shen, G. Zhang, X. Shi, *ACS Appl. Mater. Interfaces* **2014**, *6*, 17190–17199.
[42] L. E. Marbella, J. E. Millstone, *Chem. Mater.* **2015**, *27*, 2721–2739.
[43] K. R. Gopidas, J. K. Whitesell, M. A. Fox, *J. Am. Chem. Soc.* **2003**, *125*, 6491–6502.
[44] S. Chen, R. W. Murray, *Langmuir* **1999**, *15*, 682–689.

Submitted: September 10, 2019
Accepted: November 26, 2019